# A New Method for RGB to XYZ Transformation Based on Pattern Search Optimization

Simone Bianco, Francesca Gasparini, Alessandro Russo, and Raimondo Schettini

**Abstract — *In this paper we present an RGB to XYZ transformation method based on a pattern search optimization algorithm. Whatever strategy is adopted to initialize the color transformation, our method is able to optimize it in order to minimize the color error on a given training set, also taking into account a color mapping constraint. We report experimental results on simulated and real data sets showing that our method significantly outperforms existing ones.***

**Index Terms — Color space transformation, pattern search optimization, linear regression, RGB to XYZ color transformation.**

## I. INTRODUCTION

Very often color sensors in input devices are not colorimetric, in the sense that the RGB device values are not a linear transformation of the XYZ tristimulus values [1]. In order to develop a device-independent description of color for these devices, one needs to build a transformation from device RGB to the CIE XYZ tristimulus values. Several different methods exist, spacing from interpolation-based methods [2,3,4] to best fitting methods. Often for computational reasons the mapping from RGB to XYZ has to be defined by a 3×3 matrix transformation (especially for low computational devices such as digital still cameras). This transformation, called matrixing, is often defined as the best linear least squares mapping for the particular calibration set of surface reflectances under a given illuminant. The least-squares regression optimally maps RGB values to XYZ values so that the residual squared error for the calibration data set is minimized [5]. Given the importance of white (and also the gray-scale) in color reproduction, Finlayson and Drew have developed the White Point Preserving Least Squares fit (WPPLS) procedure [6]. As the name suggests, WPPLS is a method for determining the best least-squares transformation that maps the RGB values to the XYZ values subject to the constraint that the RGB corresponding to the white point is mapped without error. We underline that any constrained mapping is no longer optimal in the usual sense, since it produces larger errors (in terms of residual error) for any set of calibration reflectances used.

S. B., F. G. and R. S. are with University of Milano Bicocca, DISCo, Dipartimento di Informatica, Sistemistica e Comunicazione, via Bicocca degli Arcimboldi 8, 20126, Milano, Italy (e-mail: simone.bianco@disco.unimib.it, gasparini@disco.unimib.it, schettini@disco.unimib.it).

A. R. is with University of Milano Bicocca, Dipartimento di Matematica e Applicazioni, Via Cozzi 53, 20125, Milano, Italy (e-mail: alessandro.russo@unimib.it).

The Least Squares method (LS) uses a full rank matrix (rank-3), while a constrained LS method only uses a rank-2 matrix in order not to affect the exact mapping of the white. We could extend the constrained regression method and preserve two different colors. In this case the transformation matrix would be restricted to account for the best least-squares fit in a single direction. This direction is orthogonal to the plane spanned by the two vectors defining the color constraints. As expected, in this case the color transformation result is worse than in the case of a single color constraint. We could try to exactly map three colors, but as we are working with a 3×3 transformation matrix, we would not have any free dimension to apply LS fitting. In order to satisfy three constraints, we have to define them as the principal components of the reflectances under consideration [7,8]. With the intent of adding more information in the mapping, Vrhel and Trussel have developed the Non-Maximum Ignorance method (NonMaxIg). This method exploits not only the spectral sensitivities of the device, but also the specific nature of a real reflectance set [9].

In this paper we focus on digital still cameras and present a 3×3 RGB to XYZ transformation method exploiting a pattern search optimization algorithm [10,11,12,13,14]. This method is articulated in two steps: first, the color transformation matrix is initialized using any of the commonly used methods (Least Squares, White Point Preserving Least Squares, Non Maximum Ignorance, etc.); then this matrix is optimized in order to minimize the color transformation error on a given training set, eventually taking into account white color mapping constraints. Our optimization procedure is extremely robust as it returns the same transformation matrix whatever the initial approximation is (the coarser the approximation, the greater the number of iterations required).

In Section II we briefly introduce the color transformation methods available in the literature, while our optimization procedure is described in Section III. Section IV reports experimental results on simulated and real data sets. Finally in Section V we report our conclusions and outline future research.

## II. COLOR SPACE TRANSFORMATIONS

In this section we consider how input device RGB values can be mapped to XYZ tristimulus values. For concreteness, we shall focus the discussion on digital cameras, although the methods shown apply equally well to other input devices and other color transformations.

Contributed Paper
Manuscript received May 31, 2007

### *A. Color and Image Formation Model*

We denote the surface reflectance **s** with a q×1 vector, where q is the number of sampling points within the visible spectrum. Similarly, illuminant spectral power distribution and the spectral sensitivities of the filters of digital cameras can be represented respectively with a q×1 vector **i** and q×3 matrix $\mathbf{X} = [X_1, X_2, X_3]$, where $X_i$, i=1,…,3 are the three spectral sensitivities of the device used.

Given this representation of illuminant, reflectance, and spectral sensitivities, we can write the equation of color formation as:

$$\rho = \mathbf{X}^T D(\mathbf{i})\mathbf{s} \ , \qquad (1)$$

where $^T$ denotes the vector transpose, D(·) is an operator transforming a q×1 vector into a diagonal q×q matrix so that each diagonal element at [i,i] corresponds to the i-th element of the vector and the off-diagonal terms are all zeros, and **ρ** is the 3×1 vector of the device RGB values measured in the considered pixel [1].

### *B. Color space transformation using Least-Squares Regression*

Below, we give a formal derivation of the least-squares regression method [5]. In this method $\bar{\mathbf{X}} = [\bar{x}, \bar{y}, \bar{z}]$ is a q×3 matrix that can be made up both of sampled CIE standard observer functions or of a set of theoretical XYZ values for a given set of patches. **X**=[x,y,z] is another q×3 matrix that can be respectively made up of the spectral sensitivities of the device used or the RGB-device-dependent values for the given set of patches. In both cases, roughly speaking, **X** represents the values of the device we have and $\bar{\mathbf{X}}$ the theoretical values we would like to obtain. Assuming linear mapping, we have to find the 3×3 matrix **M** that minimizes the sum of the squared residuals:

$$\mathcal{F} = \|\bar{\mathbf{X}} - \mathbf{X}\mathbf{M}\|_2^2 \ . \qquad (2)$$

The problem is then to minimize the residual:

$$\varepsilon^2 = \sum_{i=1}^{3} \left[ \bar{X}^{(i)} - \sum_{k=1}^{3} m_{i,k} X^{(k)} \right]^2 \qquad (3)$$

where $X^{(i)}$ is the i-th column of **X**, analogously for $\bar{\mathbf{X}}^{(i)}$ and $m_{i,k}$ is the element of the matrix **M** in the position i,k. In order to minimize equation (3) we consider the square system:

$$\frac{\partial \varepsilon^2}{\partial m_{i,k}} = 0 \ , \quad k = 1,2,3 \ .$$

We show how it is possible to find a column of **M**; the others can be found in the same way.

$$\begin{bmatrix} \sum_{i=1}^{q} (X_i^{(1)})^2 & \sum_{i=1}^{q} X_i^{(1)} X_i^{(2)} & \sum_{i=1}^{q} X_i^{(1)} X_i^{(3)} \\ \sum_{i=1}^{q} X_i^{(2)} X_i^{(1)} & \sum_{i=1}^{q} (X_i^{(2)})^2 & \sum_{i=1}^{q} X_i^{(2)} X_i^{(3)} \\ \sum_{i=1}^{q} X_i^{(3)} X_i^{(1)} & \sum_{i=1}^{q} X_i^{(3)} X_i^{(2)} & \sum_{i=1}^{q} (X_i^{(3)})^2 \end{bmatrix} \begin{bmatrix} m_{1,k} \\ m_{2,k} \\ m_{3,k} \end{bmatrix} = \begin{bmatrix} \sum_{i=1}^{q} X_i^{(1)} \bar{X}_i^{(k)} \\ \sum_{i=1}^{q} X_i^{(2)} \bar{X}_i^{(k)} \\ \sum_{i=1}^{q} X_i^{(3)} \bar{X}_i^{(k)} \end{bmatrix} \qquad (4)$$

Equations (4) are also called *normal equations* of the problem. Let us consider again the whole problem of finding **M**; then the three particular equations (4) for k=1,2,3 can be written in the compact form **B M**=d. A careful consideration of the first member on the left-hand side of equation (4) leads to:

$$\mathbf{B} = \mathbf{X}^T\mathbf{X} \ , \quad \mathbf{X} = \begin{bmatrix} X_1^{(1)} & X_1^{(2)} & X_1^{(3)} \\ \vdots & \vdots & \vdots \\ X_q^{(1)} & X_q^{(2)} & X_q^{(3)} \end{bmatrix} . \qquad (5)$$

Furthermore, the right-hand side of equation (4) can be written as:

$$d = \mathbf{X}^T\bar{\mathbf{X}} \ , \quad \bar{\mathbf{X}} = \begin{bmatrix} \bar{X}_1^{(1)} & \bar{X}_1^{(2)} & \bar{X}_1^{(3)} \\ \vdots & \vdots & \vdots \\ \bar{X}_q^{(1)} & \bar{X}_q^{(2)} & \bar{X}_q^{(3)} \end{bmatrix} . \qquad (6)$$

Using equations (5) and (6), equation (4) becomes:

$$\mathbf{X}^T\mathbf{X}\mathbf{M} = \mathbf{X}^T\bar{\mathbf{X}} \qquad (7)$$

that can be solved in **M** to give:

$$\mathbf{M} = (\mathbf{X}^T\mathbf{X})^{-1}\mathbf{X}^T\bar{\mathbf{X}} \qquad (8)$$

which is the solution we are looking for.

The LS transform makes no assumptions about the surfaces that will be mapped with a low error and those that will be mapped with a high error. In particular, we do not expect the white point to be preserved, despite the importance of white for color reproduction. To ensure the correct mapping of white (or any other color we would like to constrain) we need to use the constrained least-squares regression developed by Finlayson and Drew [6].

### *C. Color space transformation using Constrained Least-Squares Regression*

In this section we use the same notation used in section II.B, so $\bar{\mathbf{X}}$ is a q×3 matrix that can be made up both of sampled CIE standard observer functions or a set of theoretical XYZ values for a given set of patches. **X** is another q×3 matrix that can be respectively made up of the spectral sensitivities of the device used or the RGB-device-dependent values for the given set of patches. According to [6], let $x^C$ denotes the device RGB vector for a constraint color (a color we want to map without error). Let $\bar{x}^C$ denotes the corresponding constraint XYZ tristimulus vector. We can ensure that the constraint color is mapped without error by augmenting equation (2) with a Lagrange multiplier term:

$$\mathcal{F} = \|\bar{\mathbf{X}} - \mathbf{X}\mathbf{M}\|_2^2 + \Lambda \sum_{k=1}^{3} \left( \bar{x}_k^C - \sum_{j=1}^{3} x_j^C m_{jk} \right) \ . \tag{9}$$

Here, Λ is a Lagrange multiplier that captures the idea that the constraint color in RGB coordinates $x^C$ must go over to the correct XYZ vector $\bar{x}^C$. Taking partial derivatives with respect to the Lagrange multiplier yields the constraint condition:

$$\|(\bar{x}^C)^T - (x^C)^T\mathbf{M}\| = 0 \tag{10}$$

and taking derivatives with respect to the elements $m_{jk}$ of **M**, we obtain:

$$\sum_{i=1}^{q} x_{ij}\left(\bar{x}_{ik} - \sum_{h=1}^{3} x_{ih}m_{hk}\right) + \Lambda \sum_{k=1}^{3} x_j^C\left(\bar{x}_k^C - \sum_{h=1}^{3} x_h^C m_{hk}\right) \ . \tag{11}$$

Clearly, the solution of equations (9) and (10) is that the constraint color is correctly mapped,

$$(\bar{x}^C)^T = (x^C)^T\mathbf{M} \ , \tag{12}$$

and **M** satisfies equation (7).
However, now **M** must be of a form that obeys the constraint (12). Any such matrix **M** must be of the form:

$$\mathbf{M} = \mathbf{D} + \mathbf{E} \tag{13}$$

with

$$\mathbf{D} = \begin{bmatrix} x_1^C/\bar{x}_1^C & 0 & 0 \\ 0 & x_2^C/\bar{x}_2^C & 0 \\ 0 & 0 & x_3^C/\bar{x}_3^C \end{bmatrix} \ ,$$

and **E** any matrix that satisfies $(\bar{x}^C)^T$ **E**=0. Every such matrix **E** can be written as:

$$\mathbf{E} = \mathbf{Z}\mathbf{N} \tag{14}$$

where **Z** is a 3 ×2 matrix composed of any two vectors $\sigma_1$ and $\sigma_2$ orthogonal to $\bar{x}^C$ and **N** is an arbitrary 2×3 matrix, so that **E** results as a 3 ×3 matrix.
Substituting equations (13) and (14) into (7), we can solve for **N** by premultiplying for $\mathbf{Z}^T$; then we have:

$$\mathbf{Z}^T\mathbf{X}^T\bar{\mathbf{X}} - \mathbf{Z}^T\mathbf{X}^T\mathbf{X}\mathbf{D} = [\mathbf{Z}^T\mathbf{X}^T\mathbf{X}\mathbf{Z}]\mathbf{N} \ . \tag{15}$$

This is exactly the normal equation one obtains, by starting from the minimization of equation (4) considering **M** as it is defined in equations (13) and (14). The matrix **M** is made up of the diagonal matrix **D** augmented by a rank-2 matrix that does not affect the mapping of the constraint color.

### *D. Color space transformation using Non-Maximum Ignorance*

Vrhel and Trussel, in [9], showed that the LS solution given in equation (8) can be written in terms of the non-mean subtracted covariance matrix (**K**, the q×q matrix of products, called cross-product matrix) of a set of reflectance data, most likely present in real scenes. If **S** is an n×q matrix, where each row represents a given reflectance spectrum, then **K** is defined as $\mathbf{K}=\mathbf{S}^T\mathbf{S}$. Thus this method exploits not only the spectral sensitivities of the device, but also the specific nature of a real reflectance set through the cross-product matrix. It is evident that a least-squares regression between camera responses and tristimulus values depends only on **K**. To show this, let us rewrite equation (8) making the role of the reflectance **S** explicit:

$$\mathbf{M} = (\mathbf{X}^T\mathbf{S}^T\mathbf{S}\mathbf{X})^{-1}\mathbf{X}^T\mathbf{S}^T\mathbf{S}\bar{\mathbf{X}} \ , \tag{16}$$

by substituting $\mathbf{K}=\mathbf{S}^T\mathbf{S}$, it becomes:

$$\mathbf{M} = (\mathbf{X}^T\mathbf{K}\mathbf{X})^{-1}\mathbf{X}^T\mathbf{K}\bar{\mathbf{X}} \ . \tag{17}$$

We can then say that for any particular LS transform **M**, any data set will share the same **M** if it has the same product matrix **K**.

The validity of this idea turns out to persist in the WPPLS calculation as well. Rewriting equation (15) and solving for **N**, we have:

$$\mathbf{N} = [\mathbf{Z}^T\mathbf{X}^T\mathbf{K}\mathbf{X}\mathbf{Z}]^{-1}[\mathbf{Z}^T\mathbf{X}^T\mathbf{K}\bar{\mathbf{X}} - \mathbf{Z}^T\mathbf{X}^T\mathbf{K}\mathbf{X}\mathbf{D}] \ . \tag{18}$$

## III. COLOR SPACE TRANSFORMATION OPTIMIZATION USING PATTERN SEARCH

In this section we report our Pattern Search Optimization method for color transformations. It has been developed to improve the results of both LS and WPPLS methods.
Let $\bar{\mathbf{X}}$ be the p×3 matrix containing the XYZ values calculated from the reflectances of the colors we would like to map with smaller errors, **X** the p×3 matrix containing the simulated RGB values calculated from the same reflectances, and **M** the color transformation matrix we want to find.
The function we want to minimize is no longer constituted by the norm $\|\cdot\|_2$ of $\|\bar{\mathbf{X}} - \mathbf{X}\mathbf{M}\|_2^2$, as in equation (2) or (9), but is replaced by the norm $\|\cdot\|_1$, $\|\bar{\mathbf{X}} - \mathbf{X}\mathbf{M}\|_1$ where we experimentally found that it conveys only slightly better results. In order to also minimize the minimum and the maximum errors which we have in color transformation (not possible with the LS and WPPLS methods), we have to add two more terms in the function we want to minimize:

min(| $\bar{\mathbf{X}}$–$\mathbf{XM}$ |) and || $\bar{\mathbf{X}}$–$\mathbf{XM}$||$_\infty$. The LS and WPPLS methods can not handle the noise amplification that may occur due to the matrixing process. In order to keep this amplification low we add in the function to minimize stdev ($\bar{\mathbf{X}}$–$\mathbf{XM}$) as the fourth term.

Thus the function we want to minimize is:

$$\mathcal{F} = \alpha \, \|\bar{X} - XM\|_1 + \beta \, \|\bar{X} - XM\|_\infty + \gamma \, \min(|\bar{X} - XM|) + \\ + \delta \, \mathrm{stdev}(\bar{X} - XM) \, , \qquad (19)$$

where α,β,γ,δ are weights that capture the relative importance of the terms to minimize.

We have chosen to use α = β = γ = δ = 1 as we do not have any ranking of the importance of the members in equation (19), but these can be changed as one prefers.

The problem is now to find a method to minimize the equation (19), subject to the additional constraint of exactly mapping the white point (i.e., the matrix M has to solve the constraint [1 1 1] M=[1 1 1]). As the first term of equation (19) is not differentiable, it is not possible to use methods that make explicit use of the Jacobian or the Hessian, such as the Quasi-Newton Line Search [15] or the Nonlinear Least Squares [16]. Furthermore the fourth term is not linear, and thus it is not possible to use methods as the Simplex or its variations [17] that work only for linear problems.

We need a method that does not explicitly make use of the derivatives of the function to minimize, nor computes or approximates them, and that does not make assumptions on the shape of the function. Our choice is then to use the Pattern Search method, which is capable of solving a great variety of problems [10].

Pattern Search Methods (PSM) are a class of direct search methods for nonlinear optimization [11]. Their popularity is given by simplicity and by the fact that they work very well in practice on a variety of problems. Furthermore, global convergence can be established under certain regularity assumptions of the function to be minimized [12,13,14]. PSM are extremely simple to implement and do not require any explicit estimate of derivatives.

The form of a general pattern search algorithm can be described in the following way. At each step k, we have the current iterate $x_k$ and a set $D_k$ of vectors which identify the search directions; usually the set $D_k$ is the same for all iterations. The last ingredient is the step-length parameter $\Delta_k$. For each direction $d_k \in D_k$, we set $x^+ = x_k + \Delta_k d_k$ (the "pattern") and we examine $f(x^+)$. If a $d_k$ exists such that $f(x^+) < f(x_k)$, we set $x_{k+1} = x^+$ and $\Delta_{k+1} = \alpha_k \Delta_k$ with $\alpha_k \geq 1$; otherwise, we set $x_{k+1} = x_k$ and $\Delta_{k+1} = \beta_k \Delta_k$ with $\beta_k < 1$.

In other words, if we find a better point in the pattern, we go there and increase the step; otherwise, we do not move and reduce the step. The algorithm stops when the step $\Delta_k$ is small enough.

It is clear that the algorithm works if we have a sufficiently rich set of directions and if there is a reasonable back-tracking strategy that avoids unnecessarily short steps. The main difference between PSM and other minimization algorithm based on estimations of derivatives lies in the restriction of the nature of the steps allowed between successive iterates. In fact, the new iterate $x_{k+1}$ is either $x_k$ or one of the points $x_{k+1}+\Delta_k d_k$. In practice this feature permits useful search strategies that are precluded by the nature of gradient-based methods, in which the search directions are not decided by the user.

The PSM used in this paper simply takes as $D_k$ the directions given by the coordinate axes and the step-length parameter is reduced or increased by a factor 2.

## IV. Experimental results

The experimental results reported refer to both unconstrained and constrained methods. Least Squares (LS), Non Maximum Ignorance (NonMaxIg) and our Pattern Search (PS) find the best solution without respecting any constraint on white reproduction. White Point Preserving Least Squares (WPPLS) and our White Point Preserving Pattern Search (WPPPS) find the best solution respecting the constraint that the white is mapped without error. In all the experiments, to initialize our optimization procedures for both unconstrained and constrained cases, we have adopted the matrix estimated by the least squares method. Our PS and WPPPS methods are iterative. Given the initialization just described the methods converge to the solution in about 1-2 minutes on a PC Intel Pentium 4 2.6GHz, 760MB of RAM, with Windows XP Professional operating system using the Pattern Search implementation furnished in the Genetic Algorithm and Direct Search Toolbox of Matlab 7.0. Using the identity matrix as initialization elevates the convergence time at the order of 1.5-2 hours. It is the case to underline that our methods are robust and whatever is the initialization used they always converge to the same identical results. However this computation has to been done only once, as the digital camera only applies this 3×3 matrix to the RGB values recorded by the sensor.

The experimental results are evaluated in two different frameworks: a simulated ideal imaging system and a real imaging system. For both systems we have adopted the D65 CIE standard illuminant [18]. The spectral sensitivities of the filters for the ideal imaging system are those of the real digital camera adopted in the second experimental framework. The results are compared in terms of the CIELAB $\Delta E_{76}$ color error [18]; the choice of using $\Delta E_{76}$ error is justified by the fact that most works on this topic have used it, and so results are easily comparable. The $\Delta E_{94}$ color error conveys different numerical results but leaves the rankings of the implemented methods unchanged.

### *A. Simulated ideal imaging system*

The experiments reported here have been performed on some 40000 reflectances [19] with the D65 CIE standard as the reference illuminant. This database has been randomly divided into a training and a test set, each of 20000 reflectances. The training set has been used for the Pattern Search optimization, and to evaluate the cross-product matrix of the Non-Maximum-Ignorance method. All the methods (whose notation is presented in Table I) have been tested on the same data set according to the following procedure (Figure 1): the tristimulus values obtained using the spectral sensitivities of the filters are mapped into the CIE XYZ color space through the transformation matrices estimated by the methods considered. These XYZ values are then compared, in terms of CIELAB color difference, with those obtained using the CIE color matching functions.

TABLE I
NOTATION ADOPTED FOR THE CONSIDERED METHODS

| Method | Notation |
|---|---|
| Least Squares | LS |
| White Point Preserving Least Squares | WPPLS |
| Non Maximum Ignorance | NonMaxIg |
| Pattern Search | PS |
| White Point Preserving Pattern Search | WPPPS |

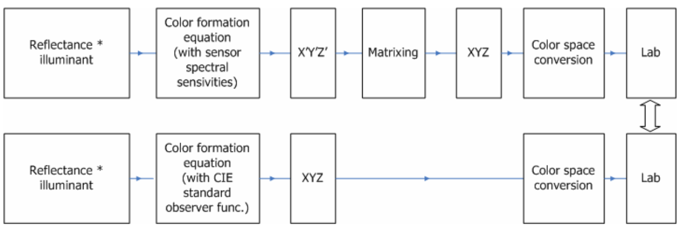


**Fig. 1. The simulated ideal imaging system under the D65 CIE standard illuminant: the tristimulus values obtained using the spectral sensivities of the filters are mapped into the CIE XYZ color space through the matrixing transformation, and then compared in terms of CIELAB color difference, with those obtained using the CIE color matching functions.**

In Tables II and III we report the statistics for the values of $\Delta E_{76}$ obtained respectively on the training and on the test sets, both of 20000 reflectances. For both, the best method is the proposed one (PS), which has the lowest values for all statistics, in particular for the mean color transformation error. Also among the constrained methods, our WPPPS shows the best results.

TABLE II
STATISTICS FOR $\Delta E_{76}$ EVALUATED ON THE TRAINING SET OF 20000 REFLECTANCES

| Matrix | Min | Max | Mean | Median | St.dev | %$\Delta E_{76}$ < 3 |
|---|---|---|---|---|---|---|
| LS | 0.36 | 62.78 | 7.69 | 7.72 | 2.78 | 2.03 |
| WPPLS | 0.34 | 143.2 | 14.98 | 12.74 | 9.61 | 2.42 |
| NonMaxIg | 0.35 | 68.45 | 7.57 | 7.49 | 2.94 | 3.87 |
| PS | 0.00 | 54.51 | 1.96 | 1.14 | 2.74 | 83.29 |
| WPPPS | 0.11 | 48.17 | 9.54 | 8.77 | 6.21 | 19.67 |

TABLE III
STATISTICS FOR $\Delta E_{76}$ EVALUATED ON THE TEST SET OF 20000 REFLECTANCES

| Matrix | Min | Max | Mean | Median | St.dev | %$\Delta E_{76}$ < 3 |
|---|---|---|---|---|---|---|
| LS | 0.48 | 71.65 | 8.44 | 8.45 | 2.87 | 1.00 |
| WPPLS | 0.47 | 167.0 | 16.87 | 14.97 | 10.36 | 1.23 |
| NonMaxIg | 0.47 | 79.94 | 8.18 | 8.14 | 3.04 | 1.36 |
| PS | 0.02 | 65.72 | 2.20 | 1.25 | 2.83 | 78.09 |
| WPPPS | 0.19 | 51.06 | 10.53 | 9.80 | 6.36 | 9.26 |

In Tables IV and V the statistics are reported using as test sets the reflectances of the Macbeth ColorChecker DC and those of the Macbeth ColorChecker CC (charts reported in Figure 2) [20]. Even if the values of the statistics are slightly changed from those of Table III, the ranking of the methods is unchanged, and our methods still show the best results (PS over all and WPPPS among the constrained methods).

TABLE IV
STATISTICS FOR $\Delta E_{76}$ EVALUATED ON THE REFLECTANCES OF THE MACBETH COLORCHECKER DC

| Matrix | Min | Max | Mean | Median | St.dev | %$\Delta E_{76}$ < 3 |
|---|---|---|---|---|---|---|
| LS | 2.57 | 72.12 | 9.78 | 9.43 | 5.41 | 0.55 |
| WPPLS | 2.40 | 179.8 | 20.15 | 17.92 | 15.28 | 1.11 |
| NonMaxIg | 2.44 | 87.37 | 9.62 | 9.31 | 6.47 | 0.55 |
| PS | 0.15 | 72.42 | 3.12 | 1.67 | 5.91 | 73.88 |
| WPPPS | 1.45 | 40.76 | 11.53 | 10.48 | 6.97 | 10.00 |

TABLE V
STATISTICS FOR $\Delta E_{76}$ EVALUATED ON THE REFLECTANCES OF THE MACBETH COLORCHECKER CC

| Matrix | Min | Max | Mean | Median | St.dev | %$\Delta E_{76}$ < 3 |
|---|---|---|---|---|---|---|
| LS | 2.61 | 72.23 | 9.81 | 9.72 | 5.50 | 4.16 |
| WPPLS | 2.47 | 175.6 | 18.92 | 15.69 | 14.92 | 8.33 |
| NonMaxIg | 2.48 | 86.72 | 9.58 | 9.23 | 6.38 | 4.16 |
| PS | 0.16 | 71.78 | 3.08 | 1.52 | 5.72 | 83.33 |
| WPPPS | 1.49 | 39.22 | 11.05 | 10.03 | 6.85 | 16.66 |

For a better comprehension of how the errors are distributed, given both the training and the test sets, we report them graphically in Appendix by means of arrows in the $a^* b^*$ plane of the $L^* a^* b^*$ space.

**Fig. 2. Left: Macbeth ColorChecker CC; right: Macbeth ColorChecker DC.**

We have also investigated the stability of the PS solution decreasing the cardinality of the training set. In Figure 3 we report the box-plots of the $\Delta E_{76}$, randomly halving the training set till it reaches 39 elements. The PS method performs almost identically from 20000 to 156 elements, as indicated by the mean values of $\Delta E_{76}$ reported in Table VI. Only at about 39 elements performance is significantly reduced.

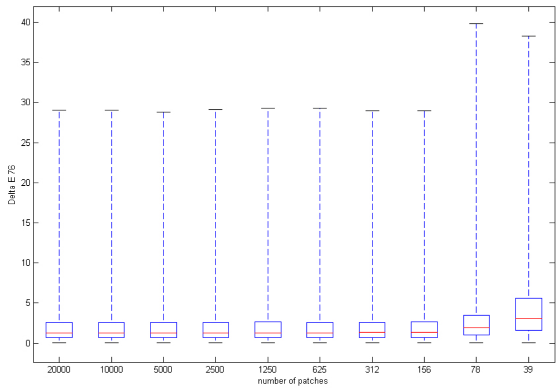


**Fig. 3. Box-plots of $\Delta E_{76}$ values for the PS method, as the number of elements in the training set decreases.**

**TABLE VI**
MEAN VALUES OF $\Delta E_{76}$ FOR THE PS METHOD, AS THE NUMBER OF ELEMENTS IN THE TRAINING SET DECREASES

| Patches | 20000 | 10000 | 5000 | 2500 | 1250 | 625 | 312 | 156 | 78 | 39 |
|---|---|---|---|---|---|---|---|---|---|---|
| $\Delta E_{76}$ | 2.15 | 2.16 | 2.15 | 2.17 | 2.19 | 2.18 | 2.17 | 2.21 | 2.73 | 4.11 |

Starting from these considerations, we have compared (Tables VII and VIII) the performance of all the methods, using as the training set the Macbeth ColorChecker DC, and as the test set the Macbeth ColorChecker CC. Note that the LS and WPPLS do not depend on a training set as they do not need to be trained. The proposed methods still perform better than the others (PS over all and WPPPS among the constrained methods).

**TABLE VII**
STATISTICS FOR $\Delta E_{76}$ EVALUATED ON THE REFLECTANCES OF THE MACBETH COLORCHECKER DC USED BOTH AS TRAINING AND TEST SET

| Matrix | Min | Max | Mean | Median | St.dev | %$\Delta E_{76}$ < 3 |
|---|---|---|---|---|---|---|
| LS | 2.57 | 72.12 | 9.78 | 9.43 | 5.41 | 0.55 |
| WPPLS | 2.40 | 179.8 | 20.15 | 17.92 | 15.28 | 1.11 |
| NonMaxIg | 2.41 | 80.23 | 9.52 | 9.20 | 6.22 | 1.11 |
| PS | 0.09 | 69.31 | 2.57 | 2.04 | 4.96 | 72.77 |
| WPPPS | 1.32 | 38.52 | 9.82 | 8.72 | 5.81 | 12.22 |

**TABLE VIII**
STATISTICS FOR $\Delta E_{76}$ EVALUATED ON THE REFLECTANCES OF THE MACBETH COLORCHECKER CC USING THE MACBETH COLORCHECKER DC AS TRAINING SET

| Matrix | Min | Max | Mean | Median | St.dev | %$\Delta E_{76}$ < 3 |
|---|---|---|---|---|---|---|
| LS | 2.61 | 72.23 | 9.81 | 9.72 | 5.50 | 4.16 |
| WPPLS | 2.47 | 175.6 | 18.92 | 15.69 | 14.92 | 8.33 |
| NonMaxIg | 2.52 | 81.37 | 10.73 | 10.21 | 6.59 | 4.16 |
| PS | 0.14 | 72.11 | 3.02 | 2.95 | 5.43 | 66.66 |
| WPPPS | 1.59 | 39.43 | 9.86 | 9.69 | 5.94 | 12.50 |

## *B. The real digital camera*

The experiments reported here have been performed using a prototype digital still camera provided by a private client. The data set used are the Macbeth ColorChecker DC and the Macbeth ColorChecker CC. The images of color charts were acquired by the camera in a standardized light-box, under the CIE D65 standard illuminant. We have used the Macbeth ColorChecker DC as the training set for the Pattern Search optimization, and to evaluate the cross-product matrix of the Non-Maximum-Ignorance method. All the methods have been evaluated, as shown in Figure 4, in terms of CIELAB color difference, on both the Macbeth ColorChecker DC and on the Macbeth ColorChecker CC. The results also include a comparison with the proprietary transformation matrix (PM), that has been provided to us by the camera manufacturer.

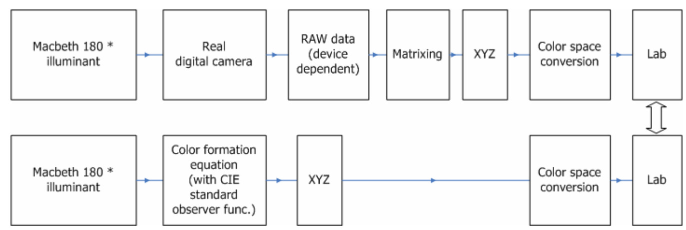


**Fig. 4. The real digital camera in the light-box under the D65 CIE standard illuminant: the RAW values acquired by the sensor of the camera are mapped into the CIE XYZ color space through the matrixing transformation, and then compared in terms of CIELAB color difference, with those obtained using the CIE color matching functions.**

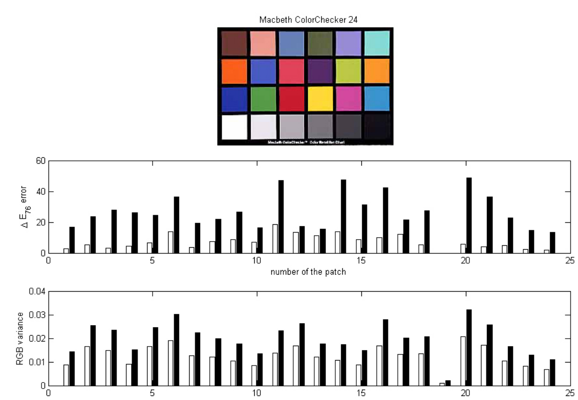


**Fig. 5. Top: the Macbeth ColorChecker CC; middle: comparison of the mean errors patch by patch of the WPPPS method (blank bars) and of the PM matrix (black bars); bottom: comparison of the standard deviation of the WPPPS method (blank bars), and of the PM matrix (black bars).**

In Table IX, the statistics for the $\Delta E_{76}$ using the Macbeth ColorChecker DC for both training and test set are reported; in Table X the same statistics are shown, using the Macbeth ColorChecker CC for test set. In both cases the PS method performs better that the others.

Applying the matrix transformation to the RAW data of a real digital camera, what we are interested in is to preserve the white. Among the constrained methods (which include the proprietary matrix PM), our WPPPS still gives the best results, even better than the unconstrained LS method.

TABLE IX
STATISTICS FOR $\Delta E_{76}$ VALUES USING AS BOTH TRAINING AND TEST SET THE MACBETH COLORCHECKER DC ACQUIRED BY THE REAL CAMERA UNDER THE STANDARD ILLUMINANT D65

| Matrix | Min | Max | Mean | Median | St.dev | %$\Delta E_{76}$ < 3 |
|---|---|---|---|---|---|---|
| LS | 1.05 | 25.19 | 7.60 | 6.84 | 4.57 | 7.78 |
| WPPLS | 0 | 30.74 | 12.76 | 12.16 | 7.25 | 4.44 |
| NonMaxIg | 0.01 | 64.65 | 37.16 | 38.07 | 12.03 | 2.78 |
| PS | 0.35 | 17.49 | 5.34 | 4.30 | 3.93 | 33.89 |
| WPPPS | 0 | 27.19 | 6.74 | 5.62 | 4.71 | 25.56 |
| PM | 0 | 61.22 | 28.83 | 26.66 | 12.27 | 4.44 |

TABLE X
STATISTICS FOR $\Delta E_{76}$ VALUES USING AS TRAINING THE MACBETH COLORCHECKER DC AND AS TEST SET THE MACBETH COLORCHECKER CC BOTH ACQUIRED BY THE REAL CAMERA UNDER THE STANDARD ILLUMINANT D65

| Matrix | Min | Max | Mean | Median | St.dev | %$\Delta E_{76}$ < 3 |
|---|---|---|---|---|---|---|
| LS | 1.44 | 27.53 | 7.61 | 7.72 | 5.13 | 12.5 |
| WPPLS | 0 | 29.08 | 13.13 | 10.57 | 7.58 | 4.16 |
| NonMaxIg | 0.01 | 53.20 | 34.38 | 34.78 | 11.05 | 4.16 |
| PS | 1.05 | 20.30 | 5.28 | 4.05 | 4.08 | 33.33 |
| WPPPS | 0 | 18.33 | 7.28 | 6.18 | 4.61 | 16.66 |
| PM | 0 | 48.56 | 26.06 | 24.00 | 12.08 | 4.16 |

In Figure 5 we report the comparison of the WPPPS method with the PM matrix in terms of the mean color error of each of the patches of the Macbeth ColorChecker CC (middle row), together with the color chart itself (top row) for a better understanding. The mean errors of the WPPPS method (blank bars) are always smaller than the corresponding ones of the PM matrix (black bars).

In the case of images acquired by real digital cameras, the noise is naturally present. The color transformation matrix may amplify this noise. Thus, for a more accurate comparison between the two methods, we also report in Figure 5 (bottom row) the standard deviation of the RGB values of each patch after transforming the RAW data applying the matrix estimated by the WPPPS method (blank bars), and the PM matrix (black bars). For all the 24 patches, the WPPPS shows a lower standard deviation.

## V. CONCLUSION

In this paper we have considered the color transformation methods available in the literature, and proposed a new one exploiting the pattern search minimization. The experimental results for both simulated and real imaging systems support the feasibility of our approach for both constrained and unconstrained color transformations. The proposed approach is quite robust and does not require that the objective function which is to be minimized is linear or differentiable. This will therefore allow us to freely design new objective functions. As further work we plan to investigate if better error functions can be defined, taking into account more color constraints, such as sets of colors that should be better reproduced than others. The Pattern Search method employed in this paper can also be greatly improved by choosing different search directions, depending on the shape of the function which is to be minimized.

We report in Figures 6,7,8,9,10 the distribution of errors in the case of the simulated ideal imaging system using the Macbeth ColorChecker DC as the training set and the Macbeth ColorChecker CC as the test set. The methods represented are the LS, PS and NonMaxIg for the unconstrained case and the WPPLS and WPPPS for the constrained case. Errors are represented by arrows. The tails of the arrows are placed in the theoretical $a^*$ $b^*$ coordinates of the patch seen under the D65 standard illuminant. The heads are placed in the $a^*$ $b^*$ coordinates in which the matrixing process has mapped the values that the simulated imaging system records for that patch.

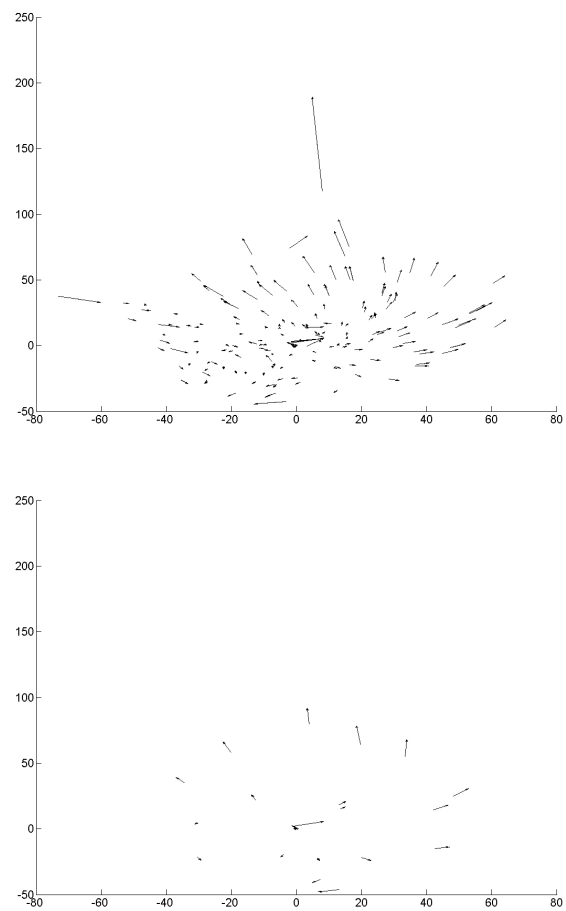


Fig. 6. Errors for the LS method; top: training set (Macbeth ColorChecker DC), bottom: test set (Macbeth ColorChecker CC).

We can notice how among the unconstrained methods (Figures 6,7,8) the error arrows for the PS method are shorter that the ones reported for the LS and NonMaxIg methods, as one could expect reading Tables IV and V. Figures 9 and 10 show much longer arrows: this is due to the fact that the errors represented are obtained by constrained methods (WPPLS and WPPPS). These methods map exactly one color point to the detriment of the overall error. The scale of the axis is now changed with respect to the Figures 6,7,8 to take into account these greater errors. Notice how also in this case our WPPPS shows a better error distribution compared to the WPPLS method.

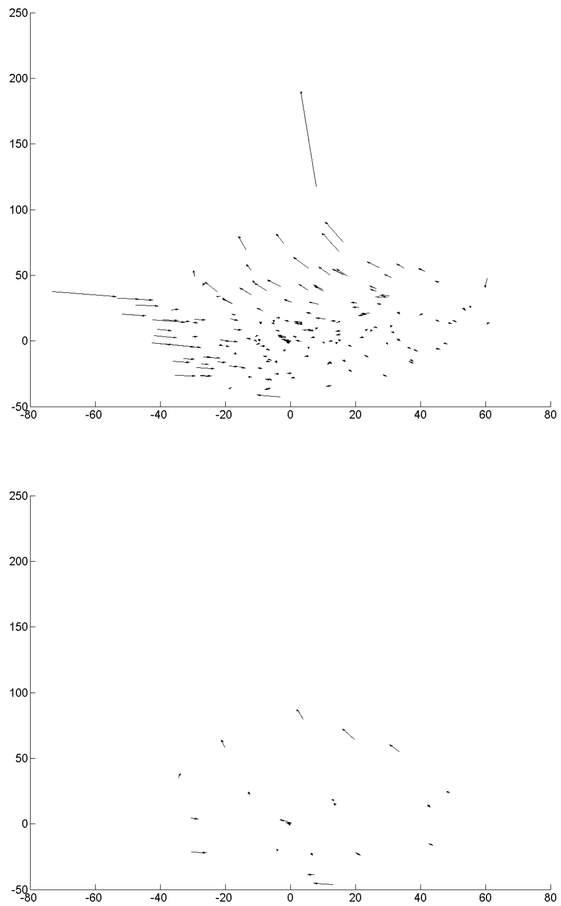


**Fig. 7. Errors for the PS method; top: training set (Macbeth ColorChecker DC), bottom: test set (Macbeth ColorChecker CC).**

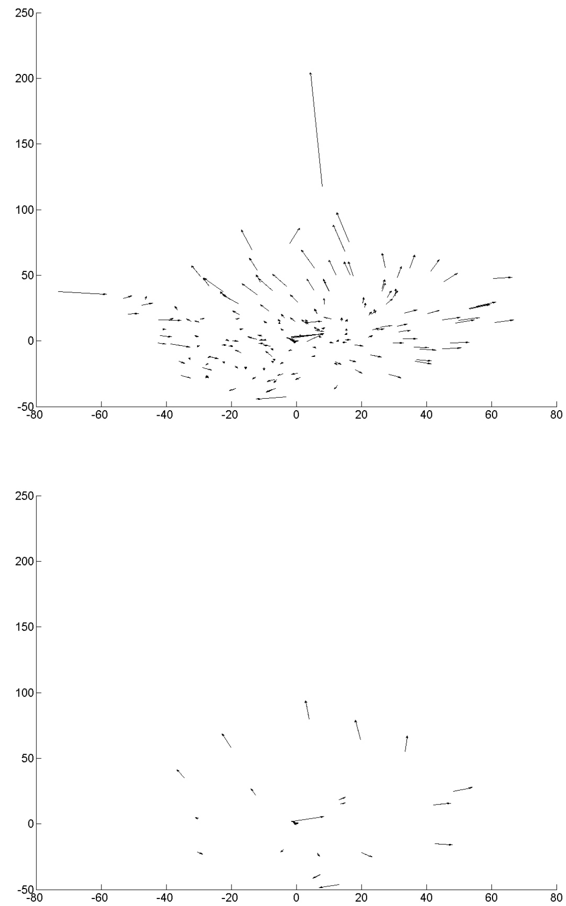


**Fig. 8. Errors for the NonMaxIg method; top: training set (Macbeth ColorChecker DC), bottom: test set (Macbeth ColorChecker CC).**

## REFERENCES

[1] G. Wyszecki, W.S. Stiles, *Color Science: Concepts and Methods, Quantitative Data and Formulas*, 2nd ed., Wiley, New York (1982).

[2] I. Amidror, "Scattered data interpolation methods for electronic imaging systems: a survey," *Journal of Electronic Imaging*, **11**, 157-176 (April 2002).

[3] P.C. Hung, "Color rendition using three-dimensional interpolation" in *Imaging applications in the Work World, Proc. SPIE* **900**, 111-115 (1988).

[4] P.C. Hung, "Colorimetric calibration for scanners and media" in *Proc. SPIE* **1448**, 164-174 (1991).

[5] G.A.F. Seber *Linear regression analysis*, John Wiley & Sons, New York (1977).

[6] G.D. Finlayson, M.S. Drew, "Constrained least-squares regression in color spaces", *J. Electronic Imaging,* **6**, 484-493 (Oct. 1997).

[7] M.J. Vrhel, H.J. Trussel, "Color correction using principal components", *Color Research and application*, **17**, 328-338 (1992).

[8] M.J. Vrhel, "Mathematical methods of color correction", PhD thesis, North Carolina State University, Department of Electrical and Computer Engineering (1993).

[9] M.J. Vrhel, H.J. Trussel, "Optimal scanning filters using spectral reflectance information" in J.P. Allebach and B.E. Rogowitz, eds., *Human Vision, Visual Processing and Digital Display IV, Proc. SPIE* **1913**, 404-412 (1993).

[10] R.M. Lewis, V. Torczon, "Why pattern search works", NASA/CR-1998-208966, ICASE Report No. 98-57 (December 1998).

[11] R.M. Lewis, V. Torczon, "On the convergence of pattern search algorithms", *SIAM Journal on Optimization*, **7**, 1-25 (1997).

[12] R.M. Lewis, V. Torczon, "Pattern search algorithms for bound constrained minimization", *SIAM Journal on Optimization*, **9**, 1082-1099 (1999).

[13] R.M. Lewis, V. Torczon, "Pattern search methods for linearly constrained minimization", *SIAM Journal on Optimization*, **10**, 917-941 (2000).

[14] R.M. Lewis, A. Shepherd, V. Torczon, "Implementing generating set search methods for linearly constrained minimization", Technical Report WM-CS-2005-01, Department of Computer Science, College of William and Mary (July 2005).

[15] D.F. Shanno "Conditioning of quasi-Newton methods for function minimization", *Mathematics of Computing*, Vol. **24**, 647-656 (1970).

[16] J.E. Dennis Jr, "Nonlinear least-squares", *State of the Art in Numerical Analysis* ed. D. Jacobs, Academic Press, 269-312 (1977).

[17] G. Dantzig, A. Orden, P. Wolfe, "Generalized simplex method for minimizing a linear form under linear inequality constraints", *Pacific J. Math.*, Vol. **5**, 183-195 (1955).

[18] http://www.cie.co.at/cie/

[19] "Graphic technology - Standard object colour spectra database for color reproduction evaluation (SOCS)", Technical Report ISO/TR 16066:2003(E).

[20] C.S. McCamy, H. Marcus, J.G. Davidson, "A color-rendition chart", *J. App. Photog. Eng.*, **2**, 95-99 (1976).

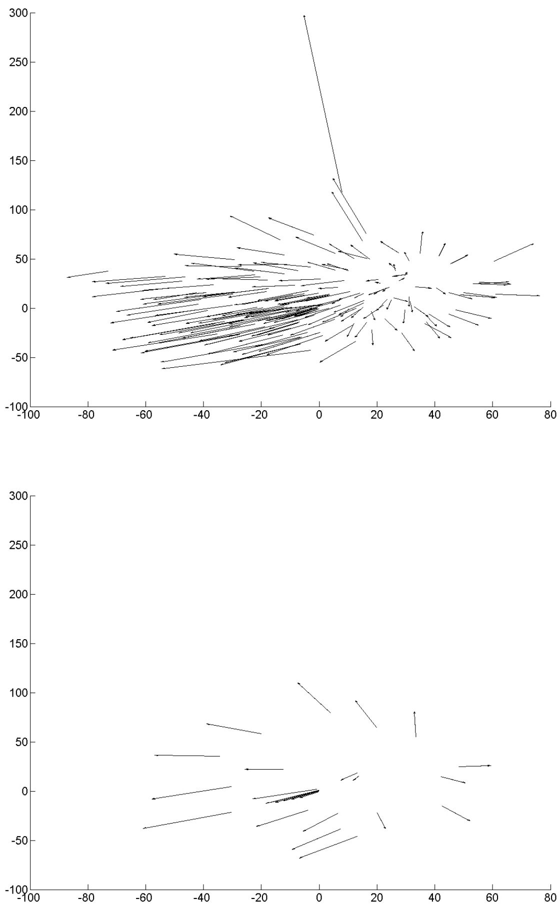


**Fig. 9. Errors for the WPPLS method; top: training set (Macbeth ColorChecker DC), bottom: test set (Macbeth ColorChecker CC).**

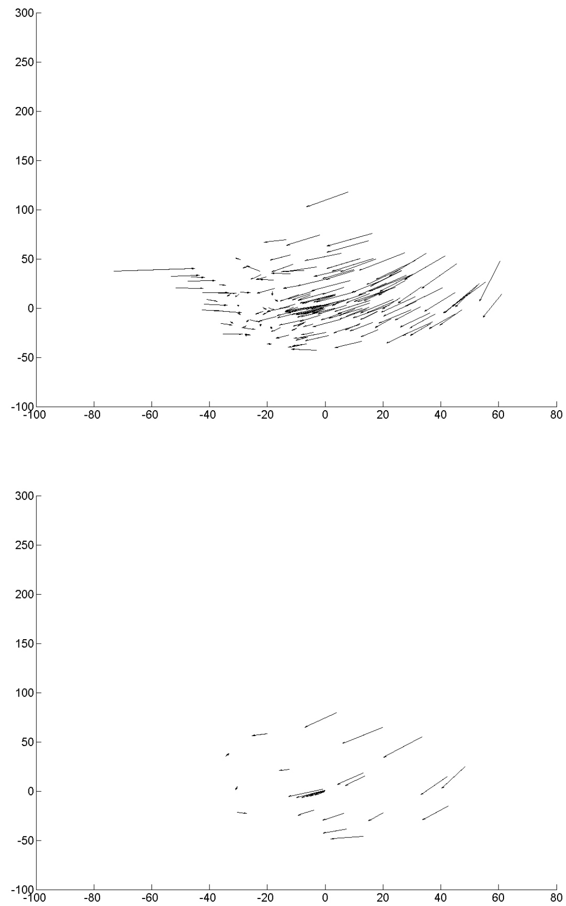


**Fig. 10. Errors for the WPPPS method; top: training set (Macbeth ColorChecker DC), bottom: test set (Macbeth ColorChecker CC).**

**Simone Bianco** was born on 13 April 1981 in Milan, Italy. He obtained the BSc and the MSc degree in Mathematics from the University of Milan-Bicocca, Italy, respectively in 2003 and 2006. He is currently a PhD student at DISCo, Department of Informatics, Systems and Communication, University of Milan-Bicocca, Italy.

**Francesca Gasparini** took her degree in Nuclear Engineering at the Polytechnic of Milan in 1997 and her Ph.D in Science and Technology in Nuclear Power Plants at the Polytechnic of Milan in 2000. Since January 2001 she has been a fellow at the ITC Imaging and Vision Laboratory, of the Italian National Research Council, located in Milan, where her research has focused on image enhancement, cast detection and cast removal. She is currently a Researcher in computer science at DISCo (Dipartimento di Informatica, Sistemistica e Comunicazione) of the University of Milano-Bicocca, working on image processing.

**Alessandro Russo** is full professor of Numerical Analysis at the Department of Mathematics and Applications of the University of Milano Bicocca

**Raimondo Schettini** is an associate professor at DISCo, University of Milano Bicocca where he is in charge of the Imaging and Vision Lab. He has been associated with Italian National Research Council (CNR) since 1987. He has been team leader in several research projects and published more than 170 refereed papers on image processing, analysis and reproduction, and on image content-based indexing and retrieval. He is an associated editor of the Pattern Recognition Journal. He was a co-guest editor of three special issues about Internet Imaging (Journal of Electronic Imaging, 2002), Color Image Processing and Analysis (Pattern Recognition Letters, 2003), and Color for Image Indexing and Retrieval (Computer Vision and Image Understanding, 2004). He was General Co-Chairman of the 1st Workshop on Image and Video Content-based Retrieval (1998), of the First European Conference on Color in Graphics, Imaging and Vision (2002), of the EI Internet Imaging Conferences (2000-2006), and of the EI Multimedia Content Access: Algorithms and Systems 2007 Conference (2007).